DISCONTINUITY WELDING DETECTION USING AN EMBEDDED HARDWARE SYSTEM

Ronald H. Hurtado, rhurtado@unb.br
Sadek C. A. Alfaro, sadek@unb.br
Carlos H. Llanos, llanos@unb.br
Facultadade de Tecnologia, Universidade de Brasília–UnB, 70910-900, Brasília-Brazil

Abstract. This paper presents the implementation of a hardware system for on-line discontinuity detection in a Gas-Tungsten arc welding process (GTAW). The hardware system is embedded in a reconfigurable device (FPGA —Field Programmable Gate Array). For case of study, a Spartan 3E 1600 from Xilinx was used. Several peripherals have been embedded into the FPGA, which implement the functionalities for developing the change detection techniques. This algorithm is divided in two modules: (a) the filtering module and (b) the stopping. In the filtering module have been described a Kalman filter, and the stopping rule module has been described a cumulative sum test (CUSUM). Additionally, other peripherals have also been included, namely a driver for the ADC, a time controller and a memory to storage the discontinuities found. Specifically, a embedded soft processor (the Microblaze) was included in order to manage the overall system for setting welding parameter, through the arc ignition until the process is complete and the discontinuity is reported. The signal, for monitoring the discontinuities, came from an infrared radiation optical sensor, which is permanently pointed out in direction to the arc. In order to validate the implementation, several tests with discontinuities, intentionally allocated in the weld bead, were made. The discontinuities include wire, holes and sand. The test results showed a good performance of the system in on-line detection for discontinuities evaluation.

Keywords: Infrared sensing, FPGA, On-line monitoring, GTAW, Embedded systems.

1. INTRODUCTION

Due the enormous quantity of variables present in the welding process (*e.g.*, current, voltage, welding velocity, flow of shielding gas) several discontinuities can occur in the weld bead. A discontinuity is referred as any typical (or expected) structural interruption of a welded joint. In this sense, a discontinuity can be considered as a lack of homogeneity in the physical, mechanical or metallurgical features of the material or weld bean. The existence of discontinuity in the joint does not necessarily mean that it is a defect. Thus, it is considered that a welded joint contains defects whenever it presents discontinuities or properties that do not meet the requirements (Modenesi, 2001).

In this context, it is very important to detect discontinuities for finding out possible fails that either could lead to structural defects or that put at risk the integrity of a structure or piece. Techniques for detecting welding discontinuities use two approaches: *off-line* and *on-line*. In the *off-line* techniques the monitoring process is achieved as a post-weld monitoring, and it is the kind of monitoring most widely used in both the laboratory as well as the industrial field. On the other hand, the *on-line* monitoring allows the user for detecting the fails or discontinuities when these appears, enabling the welding system to make corrections during the welding process and minimizing the fails, apart from reducing time and costs.

Many on-line monitoring alternatives has been proposed with interesting results (Mirapeix *et al.*, 2006; Sforza and de Blasiis, 2002). However, these techniques use a PC-platform, in which the calculation is achieved by means of a sequential execution of the instructions, apart from the operative system dependence, which introduces a over-head in the performance of the processors (Hartenstein and Kaiserslautern, 2007).

Due to the fact that the on-line monitoring welding techniques actually need real time systems for taking the appropriated actions in a suitable way, the used monitoring platform must to guarantee a good time response. This fact implies that the algorithms for monitoring and detecting discontinuities need to have a suitable performance.

Moreover, the on-line monitoring for discontinuity detection technique allows its implementation in an embedded systems (an FPGA for this case), which can accomplish good performance. Beside this, their implementations in embedded systems gives the portability option.

The embedded system design in FPGAs provides flexibility, low static and dynamic power consumption, implementing severals algorithms in parallel monitoring many signals at the same time, high-performance and reprogrammable means for implementing a variety of electronic applications. Additionally, FPGAs allow the designer to map the algorithms directly in hardware, improving its performance, when compared with their respective software implementations. Additionally, several works have reported an relevant reduction in the power consumption in the hardware implementation of the algorithms (Hartenstein and Kaiserslautern, 2007). Considering the main FPGA's characteristics, applications for monitoring several industrial process has been proposed in (de Jesús *et al.*, 2004; Fung *et al.*, 2009) Additionally, (Trejo-Hernandez *et al.*, 2010) and (Hurtado *et al.*, 2010) have proposed a methodology for on-line welding monitoring. Another important issue in the current FPGA-based embedded systems design is the *hardware/software co-design* approach.

The hardware/software co-design technique is the distribution of tasks in an application between a microprocessor component, a soft-processor for this case, running software sequentially and one or more customized hardware components (*i.e.*, co-processors) and, thus, achieving a better application performance in terms of design time, size and power consumption (Maxfield, 2009).

This paper presents an embedded hardware system based on a reconfigurable system (FPGA), that is used for discontinuity detection in a Gas Tungsten Arc Welding (GTAW) process. The infrared radiation of the voltaic arc was monitoring using an optical sensor. A hardware/software co-design approach was developed taking into account severals restrictions related to the welding platform. The developed embedded system has shown to be a suitable device for the defined application.

This paper is organized as follows: Section 2. briefly describes the background theory, where are include the Gas-Tungsten Arc Welding process and the change detection technique. Section 3. describes the issues and parts of the welding bench used and how the experimental discontinuities tests were made. Section 4. presents the hardware implementation of each module for the change detection technique and how they are connected to the MicroBlaze. Section 5. shows the results for the validation discontinuities detection tests, and finally Section 6. concludes the work.

2. BACKGROUND THEORY

2.1 Gas-Tungsten Arc Welding process

Welding is defined as the art and science of joining metals. Generally, welding includes the formation of metallurgical bonds in various kinds of fusion. In the fusion welding process, two metallic parts are joined by heating, causing the parts to melt and flow together. The heat source can be in the form of oxyacetylene flame, electric arc, electron beam, laser beam, resistive heating or combinations thereof (David *et al.*, 2003). Within the arc-welding processes is include the Gas-Tungsten Arc Welding (GTAW) which is used in this work.

In the Gas-Tungsten Arc Welding (GTAW) process the join is achieved for heating caused by the arc between the non-consumable tungsten electrode and the base material. The shielding of the electrode and the weld pool is achieved by inert gases such as helium and argon.The basic equipment consists of a power supply (CC-AC), a torch, shielding gas and an arc igniter (Modenesi and Marques, 2000).

2.2 Change detection algorithm

The change detection is a surveillance technique in which an appreciative change in the behavior of a signal y must be detected. In the context of this work, this appreciative change is called discontinuity, could mean a defect on the weld bead. In order to detect defects in welding processes an optical infrared sensor has being used. In this case, the infrared sensor measurement y_k is modeled by the Eq. (1)

$$y_k = H_k x_k + v_k \tag{1}$$

where H_k is the measurement matrix, y_k is the output of the sensor in volts, it assumes that exist a deterministic component x_k and an additive white noise v_k that has a normal distribution with mean zero and variance R, $(v_k \sim \mathcal{N}(0, R))$.

In the context of detecting changes two important concepts arise:

(a) The *estimation*, which is the task to determine the value of the variable x_k from y_k and,

(b) The *alarming* that is the fact of finding an abrupt or rapid change in x_k at time k and referred to as the *change time*.

Once the change is detected, the surveillance process is restarted to detect a new change (Gustafsson, 2000).

The related process can be considered as a linear system, and the process model in discrete time as given by Eq. (2)

$$x_k = F_{k-1} x_{k-1} + w_{k-1} \tag{2}$$

where F_{k-1} is the transition matrix from the state x_{k-1} to x_k, the random variable w_{k-1} is the process noise, having a normal distribution with mean zero and variance Q, $(w_{k-1} \sim \mathcal{N}(0, Q))$. The measurement noise v_k and the process noise w_k are not correlated. The change detection technique comprises the following three stages:

1. *filtering.*

2. *distance measurement.*

3. *stopping rule.*

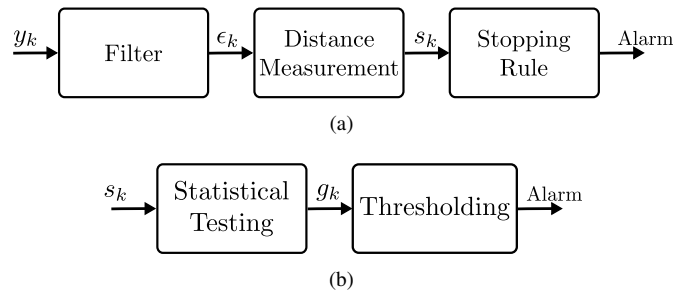These stages are depicted in Fig. 1 (Gustafsson, 2000).

Figure 1. Change detection technique block diagram. (a) Change detection based on filter result. (b) Stopping rule: statistical testing and thresholding.

2.2.1 The filtering process

In this stage a Kalman filter was used, which is an algorithm for estimating the current state $\hat{x}_k$ of a linear dynamic system perturbed for an additive white noise, using the measurements y_k (Gustafsson, 2000; Grewal and Andrews, 2001; Simon, 2006). The Kalman filter is divided in two stages, the first one is the prediction stage or *a priori* stage and the second one is the correction stage or *a posteriori* stage. In the *a priori* stage, between $k-1$ and k, the a priori estimation is represented by Eq. (3), and the a priori covariance is shown in Eq. (4)

$$\hat{x}_{k|k-1} = F_{k-1}\hat{x}_{k-1|k} \tag{3}$$

$$P_{k|k-1} = F_{k-1}P_{k-1|k}F_{k-1}^T + Q_{k-1} \tag{4}$$

In the *a posteriori* stage, the filter gain, the posteriori estimation and the posteriori covariance are calculated according to Eq. (5), Eq. (6) and Eq. (7), respectively.

$$K_k = P_{k|k-1}H_k^T \left(H_k P_{k|k-1}H_k^T + R_k\right)^{-1} \tag{5}$$

$$\hat{x}_{k|k+1} = \hat{x}_{k|k-1} + K_k \left(y_k - H_k\hat{x}_{k|k-1}\right) \tag{6}$$

$$P_{k|k+1} = \left(I - K_k H_k\right) P_{k|k-1} \tag{7}$$

2.2.2 Distance measurement

For this case, the defined distance measurements s_k are the residuals obtained from the filter according to Eq. (8)

$$s_k = \epsilon_k = y_k - \hat{x}_{k|k+1} \tag{8}$$

in which this form of s_k is appropriated whenever a change in the mean of the signal occurs.

2.2.3 Stopping rule

The stopping rule is used in surveillance to generate an alarm whenever x_k exceeds a predefined threshold h. The stopping rule comprises the *statistical test* step, which is a hypothesis test used for the alarm decision, and the *thresholding* step (Fig. 1(b)). The *statistical test* assumes one null hypothesis (there is not a change on the signal) and one alternative hypothesis (there is a change on the signal).

The cumulative sum (CUSUM) was used as part of the change detection technique. Eq. (9) shows the cumulative sum issue.

$$g_k = \max\left(g_{k-1} + s_k - \nu, 0\right) \tag{9}$$

where ν is a compensation parameter. In this case if $g_k > h$ the alarm is active and $g_k = 0$

3. EXPERIMENTAL SET-UP

This section is describe in two parts, as follow:

(a) *The welding bench*, where the instrumentation and welding tools are located and all the welding tests were made and,

(b) *The experimental discontinuities tests*, which describe how the welding tests were performed.

3.1 The welding bench

Figure 2 depicts the welding bench set-up diagram, in which the sensor, the embedded system (FPGA) and other instrumentation together with the welding tools have been allocated and all the welding tests also yielded. The main components of the welding bench are the following:

– *Positioning table*

– *GTAW welding source*
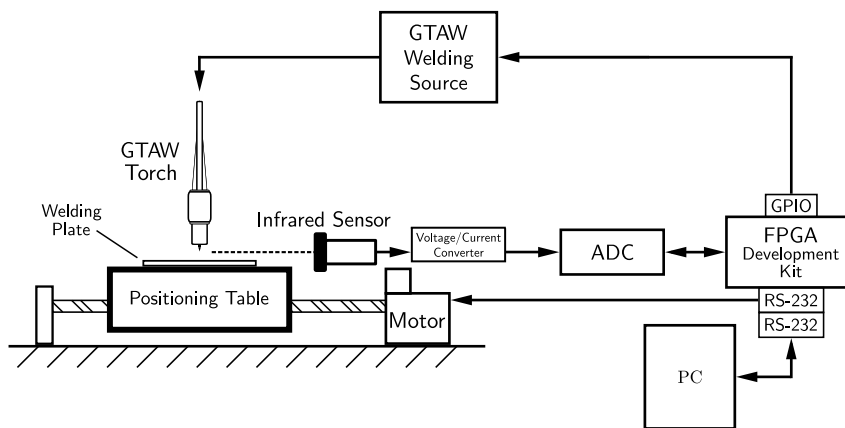
– *Infrared sensor*

– *FPGA development kit*

Figure 2. Sketch of the welding bench were the welding tests were performed.

3.1.1 The positioning table

The *positioning table* is a platform that can move linearly and where the welding plate is located and clamped. The table movement is driven by a step motor through a worm gear. The time, direction and constant velocity are adjustable parameters (Franco, 2008).

3.1.2 The GTAW welding source

The GTAW welding source used remains stationary its torch over the welding plate during the welding process with a 5 mm *stand-off*. The Inversal 450 has been the welding source used in this work.

3.1.3 The infrared sensor

The optical *infrared sensor* is a pyrometer that has its focal length to 60 cm. The sensor is allocated perpendicular to the torch in order to receive more information from the arc than the weld pool. In this work the sensor is used to measured the variation of radiation instead of the temperature in the welding process. TL-GA-18-1 from (CALEX, 2004) was the sensor used, the Tab. 1 shows some features of the sensor.

Table 1. Some technical features of the optical infrared sensor TL-GA-18-1.

Parameter	Value
Measuring	350-1800 °C
Spectral range	1,45-1,8 μm
Power supply	24 VDC
Measuring output	4-20 mmA

3.1.4 FPGA development kit

The *FPGA development kit* is based on a Spartan-3E 1600 from (Xilinx, 2007). The change detection algorithm and others customized designed peripherals have been embedded in the FPGA. To perform the management of these

peripherals (modules) and the overall welding process a soft processor has been used. The system sends to the motor the parameters (velocity and direction) and the time to be spent by the process. Additionally, the platform controls the GTAW welding source ignition, the user interface, the data exchange between the soft-processor and the customized designed peripherals.

3.2 Experimental discontinuity tests

In order to validate the embedded hardware system, developed for the discontinuity detection in a GTAW process, severals tests with intentionally introduced discontinuities in the weld bead have been performed. Three kind of discontinuities were used: *i*) *wires*, *ii*) *holes* and *iii*) *sand*. These discontinuities were located at long the weld bead in different places respect to a welding starting point.

The *wires* represents protuberances in the welding plate. These wires are based on steel alloy 1,2 mm in diameter and have been allocated perpendicular to the weld bead.

The *holes* represents the opposite to the protuberance. These hole were made along the welding plate and the diameter varies between 6 and 10 mm.

The *sand* is used as a example of *dirt spread* in the welding plate.

The welding parameters used for the tests are described in Tab. 2.

Table 2. Welding tests parameters.

Parameter	Value
Welding speed	2.5 mm/s
Weld bead length	120 mm
Shielding gas	Argon 12 l/min
Current	140 A DC
Electrode	Negative EWTh-2, 1.6 mm
Stand-off	5 mm

4. THE HARDWARE IMPLEMENTATION

This section describes the implementation or the peripherals for the change detection (Kalman filter and the CUSUM) and how they are connected to the soft-processor MicroBlaze. The change detection peripheral comprises three modules which include cores for addition/subtraction, multiplication and division operations in 32-bit floating point arithmetic (Sánchez *et al.*, 2009): (a) the *covariance&KGain* module, (b) the *estimation&error* module and (c) the *CUSUM-thresholding* module.

4.1 The *covariance&KGain* module

The *covariance&KGain* diagram is showed in Fig. 3. The Finite State Machine (FSM) is started by the input signals *En_grl* or *nextGain*. Eq. (7) is used here to calculate the covariance value to the next iteration and Eq. (5) calculates the Kalman gain, which is addressed to the output signal *KGain*.
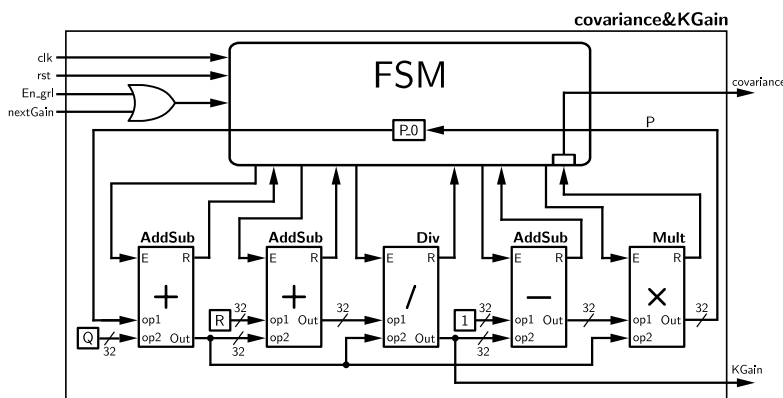

Figure 3. Architecture diagram of the *covariance&KGain* module, either started by the signal *En_grl* or *nextGain* and generating the *KGain* output.

4.2 The *estimation&error* module

The *estimation&error* diagram is shows in Fig. 4. The FSM of this unit is started by the *covariance* and *dataSet* (set-up when the data is ready) input signals. In this module is implemented the Eq. (6) to calculate both the estimation in the output signal *estimate* and its error in the output signal *erro*. The FSM activates the output signal *nextGain* during the execution of this module, thus starting calculations in the *covariance&KGain* module.
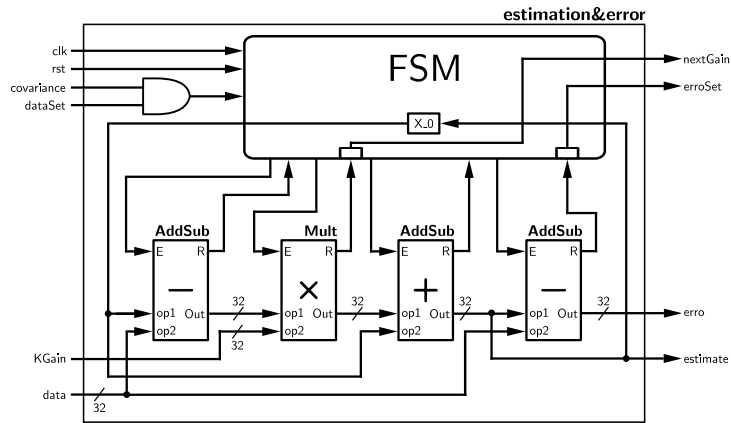

Figure 4. Architecture diagram of the *estimation&error* module that is started by *dataSet* and *covariance* signal to generate the *estimate* output.

4.3 The *CUSUM-thresholding* module

The *CUSUM-thresholding* diagram is showed in Fig. 5. The FSM of this module is started by the input signal *erroSet* and additionally calculates the cumulative sum g_h (using the input signal *erro*) and compares the result with the threshold h value according to Eq. (9). The signal *alarm* becomes active when the threshold is exceeded.
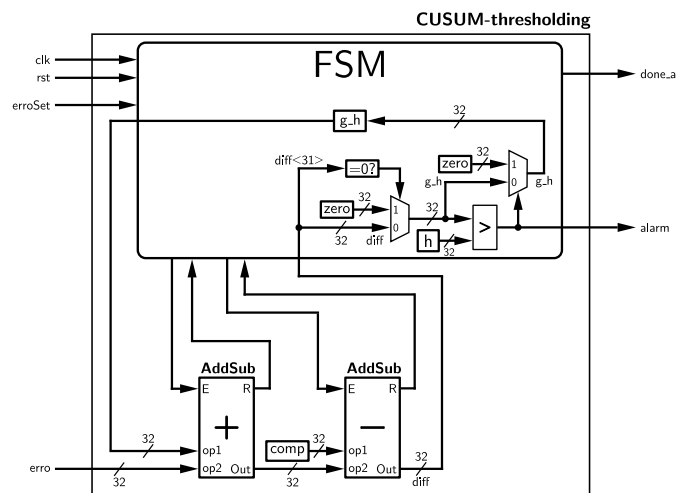

Figure 5. Architecture diagram of the *CUSUM-thresholding* module, which is started by *erroSet* signal and it generates an alarm, if it occurred, from the *erro* input.

4.4 The overall architecture

The three modules described above are condensed in *change_detector* module. Fig. 6 shows the overall architecture and the respective connections among the three modules.

According to the description of the *estimation&error* module, the *change_detector* module (showed in Fig. 6) defines a two stages pipeline structure.
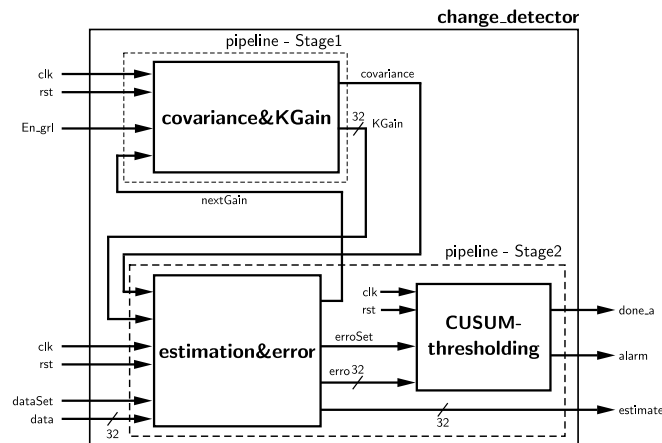
Figure 6. The change_detector block diagram, showing the way as its subcomponents (*covariance&KGain*, *estimation&error* and *CUSUM-thresholding*) are connected.

The MicroBlaze manages and communicates the described peripherals in the embedded hardware system. In order to achieved a better performance other peripheral were created and some of these were created through the EDK tool (*e.g.*, Buttons, LCD, UART) (Xilinx, 2007). These peripherals are included in the block *general purpose peripherals* (see Fig. 7). Other peripherals were custom peripherals (*i.e.*, ADC driver, time welding process manager and memory for discontinuity data). Fig. 7 depicts how the peripherals are connected to the MicroBlaze soft-processor for implementing the discontinuity welding detection system.
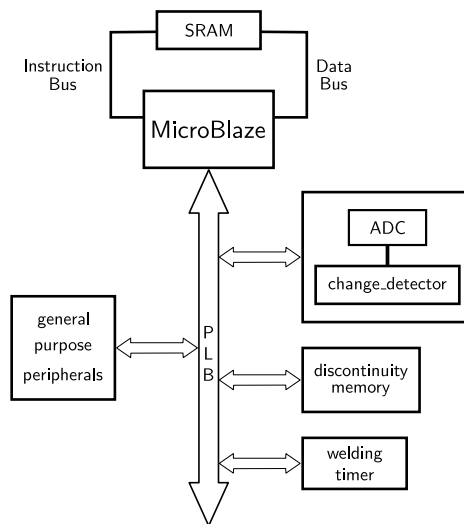

Figure 7. Architecture used for the discontinuity welding detection system, including the MicroBlaze soft-processor and the involved peripherals.

The MicroBlaze is responsible for the user interface, the selection of the welding parameters, the start of the process and the gathered information about the discontinuities (quantity and position).

4.5 The hardware consumption analysis

Table 3 shows the resources consumption for the *change_detector*, including the timing analysis, taking into account that the target used was a FPGA spartan-3E 1600 (3s1600efg320-4).

Table 3. Resources consumption synthesis for *change_detector* and its modules.

Component	Number of Slices	LUTs	MULT 18X18	Frequency (MHz)
covariance&KGain	1359 (9%)	2510 (8%)	16 (44%)	57,41
estimation&error	1043 (7%)	1916 (6%)	4 (11%)	131,88
thresholding	894 (6%)	1626 (5%)	0	129,02
change_detector	3442 (23%)	6182 (4%)	20 (55%)	57,41

The resources consumption for the overall architecture are shown in Tab. 4. The general purpose peripherals and the customized peripherals (ADC+change_detector, discontinuity memory and welding timer) are also included.

Table 4. Synthesis results for the overall architecture.

Component	Number of Slices	LUTs	MULT 18X18	Frequency (MHz)
MicroBlaze	565 (3%)	1202 (4%)	3 (8%)	95,50
ADC+change_detector	4134 (28%)	7673 (6%)	24 (66%)	39,43
discontinuity memory	358 (2%)	545 (1%)	1 (2%)	102,10
welding timer	384 (2%)	608 (2%)	0	101,74
general purpose peripherals	768 (5%)	853 (3%)	0	142,67
others peripherals	445 (3%)	670 (2%)	0	128,29

5. RESULTS

This section describes the results or each kind of discontinuity. In this case for each discontinuity a figure depicts the results as follow: in the part (a) the output signal from the infrared sensor, in the part (b) a weld bead photo and the part (c) are the alarm results for the discontinuity detection provided for the embedded hardware system.

5.1 Discontinuities by wire

Figure 8 shows a validation test where welding discontinuities has been introduced. The discontinuities were allocated, related to the welding origin, approximately at the following pair distance/wire-quantities: *i*) 25mm/1, *ii*) 45mm/2, *iii*) 80mm/3 and *iv*) 100mm/1.
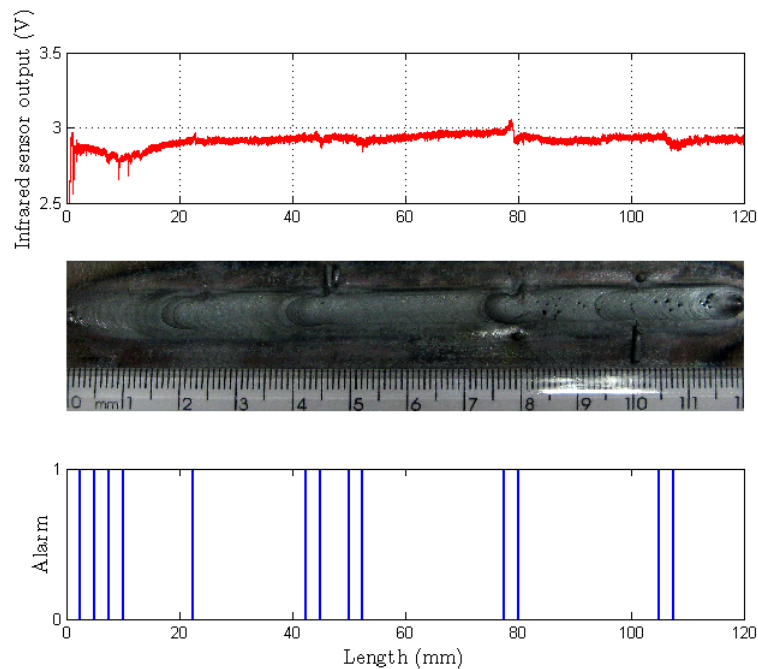

Figure 8. Discontinuities by wire. The discontinuities are generated by each pair distance/wire-quantities: 25mm/1, 45mm/2, 80mm/3 and 100mm/1.

The alarm response depicts several hits along the weld bead. For the discontinuities *ii* and *iii* the system has success and additionally detect a extrusion discontinuity. This extrusion in the weld bead is caused by the interaction between the weld pool and an additional wire material.

5.2 Discontinuities by holes

Figure 9 shows other validation tests, in this case the discontinuities are produced by holes. The discontinuities were allocated, related to the welding origin, approximately in *i*) 21-27 mm, *ii*) 50-58 mm and *iii*) 78-86 mm.
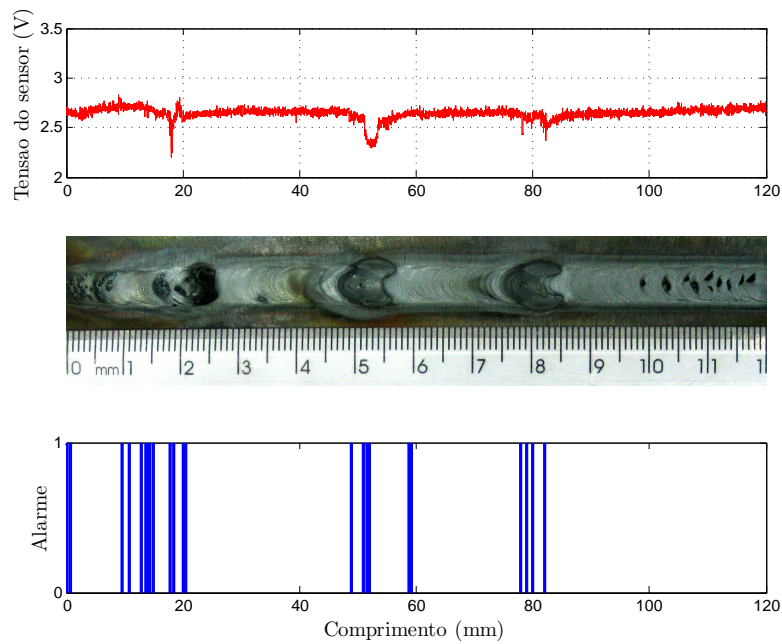
Figure 9. Discontinuities by holes. The discontinuities are located in 21-27 mm, 50-58 mm and 78-86 mm.

There are some false detection in the beginning of the weld bead, but are severals alarm hits around each discontinuities.

5.3 Discontinuities by sand

Figure 10 shows the discontinuities by the sand validation test. The discontinuities for this test were allocated, related to the welding origin, approximately between *i*) 22-35 mm, *ii*) 55-70 mm and *iii*) 90-105 mm.
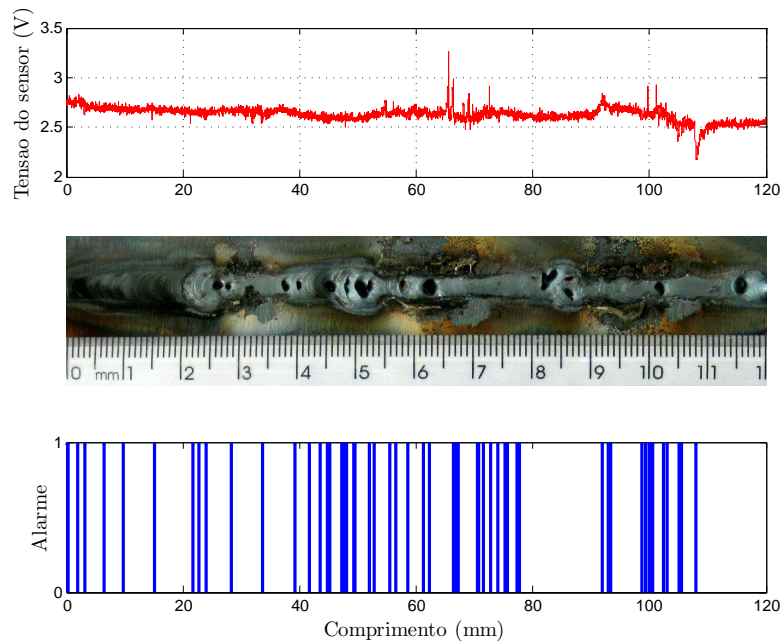

Figure 10. Discontinuities by sand. The discontinuities are located between 22-35 mm, 55-70 mm and 90-105 mm.

Severals true and false alarm hits were detected in this test, this alarms are related to the kind of discontinuity, the reject of the weld bead is justified, even by its aspect.

6. CONCLUSIONS

The implementation of an embedded hardware system for discontinuity detection in GTAW process was discussed in this paper. A Field Programmable Gate Array (FPGA) to embedded the overall hardware system was used, principally a change detection algorithm was described in it.

The synthesis results showed a low resource consumption and a overall suitable performance, considering that all of the calculation were implemented in a 32 bit floating point arithmetic, allowing to the application to guarantee a appropriate dynamic range in the arithmetic operations.

In the validation test, the discontinuities by holes were the best detected for the detection system, as long as the worse response was in the discontinuities by sand. While that in the discontinuities by wire, the alarm generation depends of the position and quantity of wire along the weld bead.

7. ACKNOWLEDGEMENTS

8. REFERENCES

CALEX, 2004. *TL-S, TL-GA – User Manual*. CALEX Electronics Ltd.

David, S.A., Babu, S.S. and Vitek, J.M., 2003. "Welding". In K.H.J. Buschow, R.W. Cahn, M.C. Flemings, B.I. (print), E.J. Kramer, S. Mahajan, and P.V. (updates), eds., *Encyclopedia of Materials: Science and Technology*, Elsevier, Oxford, pp. 1 – 9. ISBN 978-0-08-043152-9. doi:DOI: 10.1016/B0-08-043152-6/01889-1.

de Jesús, R.T.R., Gilberto, H.R., Iván, T.V. and Carlos, J.C.J., 2004. "Fpga based on-line tool breakage detection system for cnc milling machines". *Mechatronics*, Vol. 14, No. 4, pp. 439 – 454. ISSN 0957-4158. doi:DOI: 10.1016/S0957-4158(03)00069-2.

Franco, F.D., 2008. *Monitorização e Localização de Defeitos na Soldagem TIG através do Sensoriamento Infravermelho*. Master's thesis, Universidade de Brasília. Faculdade de Tecnologia. Departamento de Engenharia Mecânica.

Fung, R.F., Weng, M.H. and Kung, Y.S., 2009. "Fpga-based adaptive backstepping fuzzy control for a micro-positioning scott-russell mechanism". *Mechanical Systems and Signal Processing*, Vol. 23, No. 8, pp. 2671 – 2686. ISSN 0888-3270. doi:DOI: 10.1016/j.ymssp.2009.01.005.

Grewal, M.S. and Andrews, A.P., 2001. *Kalman Filtering: Theory and Practice Using Matlab*. John Wiley & Sons, Inc.

Gustafsson, F., 2000. *Adaptative Filtering and Change Detection*. John Wiley & Sons, Ltd.

Hartenstein, R. and Kaiserslautern, T., 2007. "Basics of reconfigurable computing". In Springer, ed., *Designing Embedded Processors*, Jörg Henkel and Sri Parameswaran, Dordrecht, The Netherlands, chapter 20, pp. 451–501. doi: 10.1007/978-1-4020-5869-1.

Hurtado, R.H., Alfaro, S.C.A. and Llanos, C.H., 2010. "A methodology for "on-line" monitoring system in a welding process using fpgas". In *Industrial Technology (ICIT), 2010 IEEE International Conference on*. pp. 162 –167. doi: 10.1109/ICIT.2010.5472672.

Maxfield, C., 2009. *FPGAs. World Class Designs*. Newnes.

Mirapeix, J., Cobo, A., Conde, O., Jaúregui, C. and López-Higuera, J., 2006. "Real-time arc welding defect detection technique by means of plasma spectrum optical analysis". *NDT & E International*, Vol. 39, No. 5, pp. 356 – 360. ISSN 0963-8695. doi:DOI: 10.1016/j.ndteint.2005.10.004.

Modenesi, P., 2001. "Soldagem i: Descontinuidades e inspeção em juntas soldas."

Modenesi, P.J. and Marques, P.V., 2000. "Soldagem i, introdução a os processos de soldagem".

Sánchez, D.F., Muñoz, D.M., Llanos, C.H. and Ayala-Rincón, M., 2009. "Parameterizable floating-point library for arithmetic operations in fpgas". In *SBCCI '09: Proceedings of the 22nd Annual Symposium on Integrated Circuits and System Design*. ACM, New York, NY, USA, pp. 253–258. ISBN 978-1-60558-705-9. doi: http://doi.acm.org/10.1145/1601896.1601948.

Sforza, P. and de Blasiis, D., 2002. "On-line optical monitoring system for arc welding". *NDT & E International*, Vol. 35, No. 1, pp. 37 – 43. ISSN 0963-8695. doi:DOI: 10.1016/S0963-8695(01)00021-4.

Simon, D., 2006. *Optimal State Estimation*. John Wiley & Sons, Inc.

Trejo-Hernandez, M., Osornio-Rios, R.A., Romero-Troncoso, R.d.J., Rodriguez-Donate, C., Dominguez-Gonzalez, A. and Herrera-Ruiz, G., 2010. "Fpga-based fused smart-sensor for tool-wear area quantitative estimation in cnc machine inserts". *Sensors*, Vol. 10, No. 4, pp. 3373–3388. ISSN 1424-8220. doi:10.3390/s100403373.

Xilinx, 2007. *MicroBlaze Development Kit Spartan-3E 1600E Edition User Guide*. ug257 (v1.1) edition.

9. Responsibility notice

The authors are the only responsible for the printed material included in this paper.